Science Translational Medicine
AAAS

www.sciencetranslationalmedicine.org/cgi/content/full/8/365/365ra159/DC1

Supplementary Materials for

The synthetic diazonamide DZ-2384 has distinct effects on microtubule curvature and dynamics without neurotoxicity

Michal Wieczorek, Joseph Tcherkezian, Cynthia Bernier, Andrea E. Prota, Sami Chaaban, Yannève Rolland, Claude Godbout, Mark A. Hancock, Joseph C. Arezzo, Ozhan Ocal, Cecilia Rocha, Natacha Olieric, Anita Hall, Hui Ding, Alexandre Bramoullé, Matthew G. Annis, George Zogopoulos, Patrick G. Harran, Thomas M. Wilkie, Rolf A. Brekken, Peter M. Siegel, Michel O. Steinmetz, Gordon C. Shore, Gary J. Brouhard,* Anne Roulston*

*Corresponding author. Email: gary.brouhard@mcgill.ca (G.J.B.); anne.roulston@mcgill.ca (A.R.)

Published 16 November 2016, *Sci. Transl. Med.* **8**, 365ra159 (2016)
DOI: 10.1126/scitranslmed.aag1093

The PDF file includes:

Other Supplementary Material for this manuscript includes the following:
(available at www.sciencetranslationalmedicine.org/cgi/content/full/8/365/365ra159/DC1)

Movie S1 (.avi format). Microtubule growing ends in U-2OS cells: vehicle control.
Movie S2 (.avi format). The effect of treatment on microtubule growing ends in U-2OS cells: DZ-2384.
Movie S3 (.avi format). The effect of treatment on microtubule growing ends in U-2OS cells: vinorelbine.

SUPPLEMENTARY MATERIALS

Materials and Methods:

Study design

The study objectives were to determine the mechanism of action of the synthetic diazonamide, DZ-2384, and to evaluate its efficacy and toxicity in several murine tumor models relative to compounds with similar mechanisms of action. Tumor models that reflected several different tumor types for which anti-mitotics are commonly used clinically were selected for evaluation. The number of animals per study, duration, and dosing frequency were selected based on prior knowledge of the growth rate and variability of each tumor model. Randomization aimed to generate treatment groups of equivalent mean tumor size or burden. One mouse was excluded from the human PDX study after initiation because its cage was flooded before randomization and it did not recover as the experiment progressed. Another animal in the same treatment group died inexplicably at day 29 but is included in the data set (as noted in the Results section). All endpoints were determined prospectively and included weight loss of greater than 20% for 3 consecutive days. Other endpoints included a sub-cutaneous tumor volume exceeding 2000 mm^3, skin ulceration, and a human CD45+ tumor proportion of > 50% of total murine and human CD45+ blood cells. The study objectives were to determine the mechanism of action of the synthetic diazonamide, DZ-2384, and to evaluate its efficacy and toxicity in several murine tumor models relative to compounds with similar mechanisms of action. Experiments investigating the mechanism of action were performed at least twice (with the exception of the siRNA screen); one representative experiment is shown. Experiments involving visual scoring of microtubule dynamics or curvature through microscopy were blinded as indicated below.

Compounds and formulations

Vinorelbine tartrate (Selleckchem) was administered to mice in saline. Docetaxel (LC Laboratories) was formulated in Cremophor EL: ethanol: saline (5:5:90) for administration to rats. Vinblastine and RO-3306 were obtained from Sigma Aldrich. Gemcitabine generic (LC Laboratories) or as Gemzar (UTSW pharmacy) was formulated in saline for administration to mice. DZ-2384 and DZ-2384D (fig. S6) were synthesized as described in Ding et al (*21*) by Paraza Pharma. DZ-2384 was formulated in Cremophor EL: ethanol: saline (5:5:90) for administration to animals.

Cell lines and viability

MIA PaCa-2, HT-29, NCI-H1299, HeLa, RS4;11, and U-2 OS cells were obtained from the American Type Culture Collection (ATCC). MDA-MB-231-LM2 (4175) cells selected for their ability to form lung metastases (*22*) were obtained from Dr. Joan Massagué. The pig epithelial kidney LLCPK1 cells, expressing GFP-α-tubulin, were obtained from Dr. Ryoma Ohi. U-2 OS cells expressing EB3-mCherry were a kind gift from Dr. Alex Bird. All cell lines were of low passage, but were not further authenticated. All cells were cultured in RPMI-1640 supplemented with 10% FBS, 100 U/mL penicillin, 100 μg/mL streptomycin, and 2 mM L-glutamine (Wisent) and maintained at 37°C in a humidified atmosphere containing 5% CO_2. U-2 OS cells expressing EB3-mcherry were also supplemented with 1mM sodium pyruvate and 40 μg/mL G418 to maintain stable protein expression. Cell viability was determined in 96-well assay plates after a 72 h treatment with test compound using the CellTiter-Glo Luminescent Cell Viability Assay (Promega) according to manufacturer's instructions. Sigmoidal dose-response curves were used to calculate the concentration of drug resulting in 50% (IC_{50}) or 80% (IC_{80}) growth inhibition (Prism v6, GraphPad).

Tumor xenograft studies

Female Crl:NU(NCr)-foxn1nu hairless mice, 4-6 weeks old (Charles River) were injected subcutaneously with MIA PaCa-2 or HT-29 cell suspensions (10^7 cells in PBS). Tumor diameters were measured with digital calipers and tumor volume estimated by: volume (mm^3) = ½ x length x $(width)^2$. Mice were randomized into groups (n=6) when tumors reached an average of 100-200 mm^3. DZ-2384 [in Cremophor:ethanol:saline(5:5:90)] or vinorelbine (in saline) was administered weekly x 4, by intravenous injection. Female CB17.Cg-$Prkdc^{scid}Lyst^{bg-J}$/Crl mice (5-6 weeks old, Charles River) were injected with $2.5x10^5$ MDA-MB231-LM2 cells in the lateral tail vein 2 weeks before treatment to allow lung metastases to establish. Lung metastases were monitored by bioluminescent imaging and mice randomized into treatment groups according to tumor burden before drug administration. Vehicle or DZ-2384 were administered intravenously (iv) twice weekly for 2 weeks and the tumor burden monitored weekly with bioluminescent imaging. The PDX subcutaneous tumor model was generated using PDA tissues obtained at the time of surgery from patients enrolled in the Quebec Pancreas Cancer Study (QPCS) (*63*). Institutional ethics approval for the QPCS includes informed consent from patients and the use of tissues to generate PDX models for in vivo studies. Fifth passage PDX fragments (1-1.5 mm^3 cubes) were implanted and expanded subcutaneously into the right and left flanks of female CB17.Cg-*Prkdc*^{scid}*Lyst*$^{bg-j}$/Crl mice (4-5 weeks old, Charles River). Mice were randomized into groups (n=5) when mean (both flanks) tumor volumes were at 60-70 mm^3 in a cohort of mice and received weekly iv injections of DZ-2384 or biweekly intra-peritoneal (ip) injections of gemcitabine for 4 weeks. All mice were weighed 2-3 times weekly throughout the experiments.

Bioluminescent imaging and analysis

Bioluminescent imaging was used to quantify the metastatic tumor burden of MDA-MB-231-LM2 cells. Briefly, 1.5 mg of D-luciferin (in PBS) was administered to mice by ip injection and animals anesthetized with 3% isoflurane. Imaging was initiated 5 min after injection with a Xenogen IVIS Spectrum system coupled to Living Image acquisition and analysis software (Perkin Elmer) at 1 min intervals for 10 min. Photon

flux was calculated for each animal by using a rectangular region of interest encompassing the thorax of the mouse in a prone position. This value was scaled to a background value from a luciferin-injected mouse with no tumor cells.

Human acute lymphocytic leukemia tumor burden

Female NOD.CB17-*Prkdc*^{SCID}*/NcrCrl* mice (5-6 weeks old, Charles River) were injected in the lateral tail vein with RS4;11 cells (8.0 x10^6 in PBS). The proportion of circulating human RS4;11 tumor cells was evaluated weekly by flow cytometry. RS4;11 tumor burden was assessed by FACS analysis of circulating tumor cells in the peripheral blood as in (*64*). Briefly, 40 μL of blood was collected weekly from each mouse (saphenous vein puncture) and pre-incubated for 10 minutes with mouse BD Fc Block antibody reagent (BD Biosciences), then stained using PE-Cy7 rat anti-murine CD45 (BD Biosciences) + FITC mouse anti-human CD45 (Tonbo biosciences) antibodies for 15 minutes. Single cell suspensions from each sample were generated using Fix/Lyse solution (eBioscience) and CD45 positive cells quantified using a FACSCalibur flow cytometer (BD biosciences). When mean counts of human CD45+ (hCD45+) cells circulating reached 2% of the total of murine and hCD45+ve cells, mice were randomized into treatment groups (n=8). Mice were treated twice weekly with vehicle or DZ-2384 iv for 2 weeks.

PDA GEMM rapid in vivo assay (Rgs16::GFP;KIC model)

Rgs16::GFP;KIC mice were maintained on normal chow *ad libitum. Rgs16::GFP;KIC* mice were identified by genotype p48::Cre and LSL-Kras^{G12D} via PCR from tails collected at P12-P13 as described (*24*). DZ-2384 and gemcitabine were administered ip once weekly for DZ-2384 and three times weekly for gemcitabine. Pancreatic tumors from *Rgs16::GFP;KIC* mice were quantified by GFP fluorescence at P29 according to the method described in (*24*). Because this model is highly consistent over time, mice in untreated and single agent gemcitabine cohorts used as comparators were enrolled within a few weeks and months of the DZ-2384/gemcitabine cohort [Supplementary fig. 10 of (*24*)],and 8 untreated mice were simultaneously enrolled. Mice

that were simultaneously enrolled were weighed once weekly. For statistics, linear scale intensity values were converted to Log_{10} and averaged for each mouse. Mean tumor burden values between two groups were compared via Student's unpaired two- tailed t-test with Welch's correction.

Determination of mouse bone marrow toxicity

Bone marrow was prepared by flushing the contents of femurs removed from euthanized mice with 100% FBS followed by smearing a thin layer of cells on a glass slide that was gently air dried with a fan. Bone marrow smears were stained with Modified Wright's stain. The myeloid to erythroid (M/E) ratio is a quantitative determination arrived at by performing a differential cell count on 200 cells.

Pharmacokinetics and compound analysis by LC-MS/MS

DZ-2384 or vinorelbine were administered as a single dose iv to female Crl:NU(NCr)-foxn1nu hairless mice (n=3) or to female Sprague Dawley rats (n=3), and blood samples were taken at 0', 5', 15' 30', 1 h, 2 h, 4 h, 8 h, and 24 h. DZ-2384 and vinorelbine were extracted from plasma with 2 volumes of acetonitrile containing the internal standard labetalol. After vortexing and centrifugation (5 min at 15,000 rpm), 20 μL of supernatant was transferred into an HPLC plate, and 2 volumes of water + 0.2% formic acid were added. Samples were analyzed in MRM mode by LC/MS/MS (AB/SCIEX 4000 QTRAP, Agilent 1100 series HPLC system) using a Luna C8(2), 30 x 2 mm, 5 mM column and a flow rate of 0.70 mL/min. Mobile phase was A: H_2O + 0.1% formic acid, B: 20/80 isopropanol/acetonitrile + 0.1% formic acid with a gradient of 10-98% B in 1.5 min, plateau at 98% B for 1.9 min. DZ-2384 and vinorelbine were quantified relative to standard curves. PK parameters were calculated using PK Functions for Microsoft Excel. Results represent the mean values for three mice per dose group.

Determination of rat maximum tolerated dose

Female Sprague-Dawley rats (7-9 weeks old) were iv administered docetaxel or DZ-2384 formulated in 5% Cre: 5% EtOH:90% saline once weekly for 4 weeks, and body weights were measured three times per week. The maximum tolerated dose is the dose at which there was no death and rats did not experience more than a 20% weight loss for more than 3 consecutive days.

Neuroelectrophysiological assessments and toxicokinetics

Neuro-toxicology experiments were conducted at CiToxLAB, Montreal, QC. Female Sprague-Dawley rats (n=12 per group) received vehicle, DZ-2384, or docetaxel once weekly for 4 weeks. Neuroelectrophysiological assessments (n=7) were made before initiation of dosing, 2 days after the last treatment (Day 24), and from recovering rats (n=5) at the end of the recovery period (Day 44). For neuroelectrophysiology, rats were anesthetized with 2% isoflurane and placed in a prone position. The active, reference, and ground electrodes were positioned with respect to bony landmarks in each animal. Platinum needle electrodes (Grass-Telefactor Co.), with impedances of approximately 50 kohms @ 1,000 Hz were used as both active and reference leads for all recordings. Neuroelectric signals were impedance matched, appropriately band-passed using multi-pole filters, and differentially amplified using a gain factor of 500 (motor) or 20 K (sensory and spinal). Data were processed using a BIOPAC 150 system with AcqKnowledge v3.8.1 (Goleta). The amplified signal was time-locked to the evoking stimulus and digitized at a rate of 1,000 Hz. Onset latencies were measured from the stimulus artifact to the initiation of the depolarization and expressed to the nearest 0.01 msec. Amplitude was measured from baseline to the peak of the depolarization to the nearest 0.01 μV for sensory responses, and to the nearest 0.01 mV for motor responses.

Study Approval

All animal experiments were performed in strict accordance with the Canadian Council on Animal Care (CCAC) and McGill University Animal Care committee guidelines or according to the rules and standards of UT Southwestern Institutional Animal Care and Use Committee.

Genome-wide synthetic lethal screen

NCI-H1299 cells (250 cells) were reverse transfected with the On-Target Plus SMARTpool siRNA library (Dharmacon, human genome-wide) at a final concentration of 20 nM using 0.0125 μL of RNAiMAX transfection reagent (Life Technologies). Automated transfections were carried out in black, clear bottom-384 plates (4 replicates x 3 plates for each pool of siRNAs) using a BioMek FX liquid handler (Beckman Coulter). SiRNA smart pool controls were included on every plate: non-targeting siNT (D-001810-10-20) and transfection controls siPLK-1 (L-003290-00) and siKif11 (L-003317), as well as a sensitizing siRNA positive control siMCL1 (L-004501). Forty-eight h after transfection, cells were treated with vehicle or DZ-2384 doses ranging from 3 μM to 0.051 nM (0.2% final DMSO). Each plate contained 4 extra wells of siNT transfected cells treated with vehicle only, which served as reference wells for normalization between plates. Three days after treatment, cell viability was measured using the CellTiter-Glo Cell viability assay according to manufacturer's instructions. Data normalization occurred by dividing raw data values in each well by the median of the siNT transfected, vehicle-treated wells of each respective assay plate.

All plates had a minimum transfection efficiency of 90% as determined using siPLK-1 and 80% using siKIF11 control. All siRNAs that produced a growth inhibition of >80% (in DMSO-treated samples) were excluded from the analysis (lethal siRNAs). The viability ratio for the remaining test siRNAs treated at each dose of DZ-2384 was calculated according to the formula below.

Viability ratio test siRNA [DZ-2384] =
Normalized viability test siRNA [DZ-2384]/
Normalized viability test siRNA [DMSO]

The calculated viability ratios for each test siRNA were then used to generate a five-parameter logistic fit IC_{50} values using the R package *drc* (v2.3). The relative differences in sensitivity to DZ-2384 for each test siRNA were expressed as the log difference in IC_{50} values between test siRNAs and the mean of two NT controls per plate.

Cell cycle and apoptosis analysis

For synchronization in late G_2 phase, H1299 cells ($5x10^5$) were incubated for 24 h with 9 μM of RO-3306 (Sigma; SML0569) (*65*). The cells were then released by replacing the medium with fresh complete medium containing vehicle or DZ-2384 for the indicated times. Cells were stained with propidium iodide and FACS analysis performed as in (*66*). Caspase 3 activation (apoptosis) was visualized by western blotting with antibodies recognizing full length and cleaved caspase 3 (Cell Signaling cat#9662 and cat#9661, respectively). Vinculin (Sigma cat#V9131) was used as a loading control.

Biotinylated diazonamide Compound Synthesis

DZ-2384 and DZ-2384D (fig. S6) were synthesized from synthetic intermediates **5** and **6**, respectively (see below). Those materials were prepared by Paraza Pharma Inc. using the methods of Ding et al. (*21*) and supplied as a 2.9:1 mixture of diastereomers favoring **5**. Biotin-labeled DZ-2384 and DZ-2384D were synthesized from intermediates **5** and **6** (vide infra) using polyfunctional biotin-containing reagent **1**

(prepared according to methods outlined in Tae et al. (*67*) and the procedures outlined below.

Preparation of compound 2. To a solution of the biotinylated reagent 1 (123 mg, 0.139 mmol) in CH_2Cl_2 (9 mL) was added trifluoroacetic acid (TFA) (3 mL). The resulting mixture was stirred at room temperature (rt) for 100 min, concentrated, co-evaporated with MeOH (2 x 10 mL), and dried. The residue was dissolved in anhydrous N, N-Dimethylformamide (DMF) (1 mL) and treated with 1-[Bis(dimethylamino)methylene]-1H-1,2,3-triazolo[4,5-b]pyridinium 3-oxid hexa-fluorophosphate (HATU) (60 mg, 0.153 mmol), 4-pentenoic acid (15.5 mg, 0.154 mmol) and N, N-Diisopropylethylamine (DIPEA) (0.1 mL, 0.557 mmol). After stirring at rt for 2 h, the reaction was quenched with saturated aqueous NH_4Cl (5 mL) and extracted with EtOAc (2 x 30 mL). The combined organic layers were washed with water (3 x 20 mL) and brine (1 x 20 mL), dried over $MgSO_4$, and concentrated under reduced pressure. Crude 2 was obtained as a colorless oil (72 mg). LRMS-ESI m/z calculated for $[C_{43}H_{59}N_7O_{10}S+H]+$: 866.4; found: 866.4.

syn and anti-Ethyl 2-hydroxy-3-methylpent-4-enoate (3). A 50 mL Schlenk tube was charged with ethyl glyoxylate (freshly distilled from a commercial 50 wt% solution in toluene (Fluka), 660 mg, 6.47 mmol) and CH_2Cl_2 (20 mL) and cooled to –78 ˚C. Me_2AlCl (1.0 M in hexanes, 6.5 mL) was added. Gaseous cis-2-butene (5.7 g, 101.7 mmol) was condensed into the solution at -78˚C (metered by cylinder weight). The Schlenck tube was sealed, and the mixture was slowly brought to room temp over 2 h. Stirring was continued overnight. The resultant mixture was re-cooled to –78˚C and treated with MeOH (1 mL). After 15 min, the mixture was warmed to room temperature, and water was added dropwise. After concentration, the residue was partitioned between Et_2O and 0.1 M HCl. The aqueous layer was extracted with Et_2O and the combined organics were washed with water, saturated $NaHCO_3$, and brine, dried over $MgSO_4$, and concentrated under reduced pressure (150 mbar, 40˚C) to give compounds 3 as a racemic mixture of diastereomers (200 mg, 1.1:1 syn/anti, 20% yield). Data for the mixture were fully consistent with those obtained on individual diastereomers: for (±)-syn-3, see (*68*); for (±)-anti-3, see (*69*).

Cross metathesis product 4. A solution of crude 2 (20 mg, 0.023 mmol), ethyl 2-hydroxy-3-methylpent-4-enoate (3) (108 mg, 0.68 mmol; d.r. = 1.1:1), and the 2nd-generation Grubbs metathesis catalyst (Grubbs II) (5.6 mg, 0.0066 mmol) in CH_2Cl_2 (1.6 mL) was stirred in a sealed vial at 40˚C for 18 h. A second portion of 3 (20 mg, 0.127 mmol) and metathesis catalyst (5.5 mg) was added, and the mixture was stirred at 40˚C for another 2 h. The solvent was removed using a stream of argon, and LiOH•H_2O (10.0 mg, 0.238 mmol) in 4:1 MeOH-H_2O (0.4 mL) was added. The mixture was stirred at rt for 1 h, treated with 1 M HCl (0.3 mL), and the resultant product solution purified by preparative HPLC to afford carboxylic acids 4 (4.1 mg, d.r. = 1.1:1). LRMS-ESI m/z calcd for $[C_{47}H_{65}N_7O_{13}S+H]+$: 968.4; found: 968.4. HPLC method: Sunfire C18 column (19 x 250 mm); 40-45% ACN in H_2O w/ 0.1% TFA, 2-7 min; 20 mL/min; monitoring at 280 nm. See fig. S13.

Biotinylated DZ-2384 and biotinylated DZ-2384D. Synthetic intermediates **5** and **6** (1.5 mg, 0.0028 mmol, d.r. = 2.9:1), HATU (1.5 mg, 0.004 mmol), carboxylic acids **4** (2.4 mg, 0.0025 mmol), and N-methylmorpholine (NMM) (7 mL, 0.59 M, 0.0042 mmol) were dissolved in anhydrous DMF (0.11 mL) and stirred at rt for 20 h. The reaction was diluted with MeOH (~ 2 mL) and purified by preparative HPLC. HPLC method: Sunfire C18 column (19 x 250 mm); 40-60% ACN in H_2O w/ 0.1% TFA, 2-9 min; 20 mL/ min; monitoring at 280 nm. Two fractions of biotinylated DZ-2384 were collected at t_{ret} = 6.8 and 7.1 min, respectively. A single fraction of biotinylated DZ-2384D was collected at t_{ret} = 7.4 min. The lineage of these materials as derived from either **5** or **6** was confirmed by repeating the coupling of **4** individually with HPLC-purified **5** or **6**. Product fractions having the same retention times were obtained in each case. Surface plasmon resonance experiments used the t_{ret} = 6.8 min and 7.4 min fractions (concentrated to dryness on Speedvac and re-dissolved in DMSO) as 'biotinylated DZ-2384' and 'biotinylated DZ-2384D,' respectively. A total of 1.4 mg of the t_{ret} = 6.8 min fraction and 0.7 mg t_{ret} = 7.4 min fraction were obtained: **biotinylated DZ-2384**: LRMS-ESI *m/z* calculated for $[C_{76}H_{91}FN_{12}O_{17}S+H]^+$: 1495.6; found: 1495.6; **biotinylated DZ-2384D**; LRMS-ESI *m/z* calculated for $[C_{76}H_{91}FN_{12}O_{17}S+H]^+$: 1495.6; found: 1495.6. See fig. S14.

Surface plasmon resonance (SPR)

Binding between DZ-2384 (1496 Da biotinylated) and tubulin (110 kDa dimer) was examined on a BIACORE T200 system (GE Healthcare) at 25°C. A tubulin-compatible running buffer (80 mM PIPES pH 6.9, 50 mM KCl, 5 mM $CaCl_2$, 0.05% (v/v) Tween-20) containing 5% (v/v) DMSO was used to capture biotinylated DZ-2384D (inactive) and DZ-2384 (active) in adjacent flow cells on streptavidin-coated sensors (10 μL/min). To test binding specificity, buffer blanks, BSA, actin, and tubulin were titrated (0 – 10 μM; 2-fold dilution series) over the immobilized surfaces in single-cycle kinetics mode (25 μL/min). To assess the binding site, 3 μM tubulin was injected in the presence of increasing competitor (DZ-2384, DZ-2384D, or vinorelbine) concentrations in multi-cycle kinetics mode (25 μL/min). Between sample injections, surfaces were regenerated at 50 μL/min using PIPES running buffer containing 1 M NaCl and 0.5% (v/v) Empigen. SPR data were double-referenced and subjected to DMSO solvent correction (in T200 Evaluation software); sensorgrams are representative of duplicate injections acquired from two independent trials.

X-ray crystallization, data collection, and structure solution

Crystals of T_2R-TTL were generated as described previously (*29*, *16*). Suitable T_2R-TTL crystals (*29)* were incubated overnight in reservoir solutions supplemented with 5 mM DZ-2384 and 18% glycerol as cryoprotectant. Crystals were then flash cooled in liquid nitrogen. DZ-2384-T2R-TTL DZ-2384 data were collected at beamline X06SA at the Swiss Light Source (Paul Scherrer Institut, Villigen PSI). Images were indexed and processed using XDS (*70*). Structure solution using the difference Fourier method and refinement were performed using the PHENIX package (*71*). Model building was carried out iteratively using the Coot software (*72*). PyMOL was used for figure preparation (The PyMOL Molecular Graphics System, Version 1.5.0.5. Schrödinger, LLC). Data collection and refinement statistics are given in table S7. Measurements of radii and pitches of helical super assemblies of different T_2R-TTL complexes were performed as previously described (*31*). Briefly, helical oligomers were obtained by superimposing T_2R-TTL complexes as follows: the α1β1 moiety of the nth complex was superimposed

onto the α2β2 moiety of the (n−1)th complex by keeping the final model as (α1β1)1, (α2β2)1, (α2β2)2, …, (α2β2)n. The radii and pitches were measured taking the RB3 helices as a reference.

Microtubule curvature quantitation and electron microscopy

8 μM MAP-rich (Cytoskeleton Inc.) or purified tubulin (see below) was mixed with 10 μM of DZ-2384 or vinblastine and 1 mM GTP in BRB80 (as above). After incubation at 37 °C for 30 mins, the sample was pipetted onto glow-discharged copper grids and stained with 0.75% uranyl formate. Grids were loaded onto a Tecnai T20 electron microscope (FEI), and images were recorded on a Gatan 4k x 4k (Gatan, Inc.) camera at 80,000x magnification, with a pixel size of 1.4 Å. The curvature of tubulin oligomers was measured using "Kappa", a custom software package for measuring the curvature (κ) of objects in biological image data. Kappa is available for download on GitHub (https://github.com/kevanlu/Kappa). The software uses a point-click method to trace an object, in this case an oligomer of tubulin in an EM image. The traces of the objects are represented by cubic B-splines, which are functions comprised of piecewise degree-3 Bézier curves (*45*) where curvature and length can be easily calculated. Images were assigned random numbers for a blinded analysis by 3 independent researchers. Each researcher traced at least 150 oligomers per condition. The output of the Kappa software is the point-by-point curvature and length of each oligomer. A custom MATLAB (MathWorks) script was written to reassign the dataset to the correct conditions and to average the point-by-point curvature values from individual oligomers. 10% of the length of each oligomer at the ends was excluded from the curvature analysis to avoid edge-specific artifacts. Images were measured by three independent evaluators who were blind to sample identification.

Microtubule sedimentation assay

H1299 cells were treated with the indicated concentrations of vehicle, DZ-2384, DZ-2384D, vinorelbine, or docetaxel for 4 h. Crude microtubule network isolation was performed as described in (*73*). Tubulin was visualized in each cell fraction by western

blot analysis. Ponceau Red (Sigma) staining of the membrane was used to visualize total protein loaded.

Confocal microscopy

U-2 OS cells and HeLa cells were seeded on poly-L-lysine glass coated coverslips. HeLa cells were synchronized for 24 h in presence of 9 μM of RO-3306 and released from G2/M phase arrest in DMSO, DZ-2384, or vinorelbine 1 h before immunofluorescence labeling. U-2 OS cells were treated with compound for 2 h before immunofluorescence labeling. Cells were fixed in 10% formalin, washed, and permeabilized in 0.2% Triton X-100 followed by blocking in 5% BSA/PBS. Cortical neurons were dissected from embryonic rat (E18) brains, dissociated with trypsin, and plated in Neurobasal medium (Invitrogen, supplemented with 2% B-27, 1% N2, glutamine, and penicillin/streptomycin) onto poly-L-lysine coated glass coverslips. Cells were fixed with cold methanol and permeabilized with 0.1% Triton, then blocked with 1% BSA/5%FBS/PBS. Tubulin staining was done with anti-α-tubulin (Sigma), then goat anti-mouse Alexa488, (Life Technologies). Where indicated, actin was stained with Phalloidin AF555 (Life Technologies) and DNA with DAPI (4',6-diamidino-2-phenylindole, dihydrochloride). Slides were mounted in ProLong gold or Vectashield medium (Vector Laboratories) and imaged with a Leica SP8 or Zeiss LSM510 confocal microscope.

Live cell imaging and microtubule dynamics

Live cell imaging of LLC-PK1 (GFP- α-tubulin) was performed using a Quorum WaveFX-X1 spinning Disc confocal system on a Leica DMI6000 B inverted fully motorized microscope connected to a Hamamatsu “ImagEM” EM-CCD camera. Image acquisition started 3 to 11 minutes (1 capture every 3 seconds for 1 minute) after drug addition to LLCPK1 cells in an environmentally controlled system in phenol red free medium. Images were assigned random numbers, and parameters of microtubule dynamics were evaluated as described (*35*) in a blinded fashion. Five individual microtubules from at least four different cells in each experiment (n=4) were selected;

only growing and/or shortening microtubules were chosen. Dynamics were quantified using image J and parameters acquired by microscopy.

Live cell imaging of microtubules growing ends

U-2 OS cells expressing an EB3-mCherry fusion protein (a kind gift from Dr. Alex Bird, MPI Dortmund) were maintained in RPMI, 10% FBS, 10 mM HEPES, 1 mM sodium pyruvate, penicillin/streptomycin, and 40 μg/mL G418. Live cell imaging of microtubules' growing ends was performed using a Quorum Wave FXX1 spinning Disc confocal system on a Leica DMI6000 B inverted fully motorized microscope connected to a Hamamatsu "ImagEM" EM-CCD camera. Cells were maintained in an environmentally controlled chamber and image acquisition started 3 minutes (1 capture every 3 seconds for 1 minute) after drug treatment.

Total internal reflection fluorescence microscopy and preparation of microscope chambers

Tubulin was purified from juvenile bovine brains using a modified version of the high-PIPES method (*74*), wherein the first polymerization cycle was performed in 100 mM PIPES instead of 1 M PIPES. Labeling of tubulin with tetramethylrhodamine (TAMRA) and Alexa Fluor-488 succinimidyl esters (Life Technologies) was as described in (*75*). GMPCPP-microtubule seeds were prepared and microscope setup/image capture performed as in (*36*). In brief, a cover glass was cleaned and silanized, and GMPCPP microtubules adhered to the silanized glass slides as described in (*76, 77*). Microtubule growth from GMPCPP seeds was achieved by incubating flow channels with tubulin in BRB80 buffer supplemented with 1 mM GTP, 0.1 mg/mL BSA, 1% 2-mercaptoethanol, 250 nM glucose oxidase, 64 nM catalase, 40 mM D-glucose. Time lapse image sequences were acquired at 10 s intervals.

Statistical analysis

Graphs were plotted and all statistical tests were performed in GraphPad Prism v.6. Results shown graphically are mean +/- SEM unless otherwise noted. Statistical differences were determined using an unpaired, non-parametric Student's t-test (Welch's) at a specific day upon experiment termination as indicated. Statistical significance for Kaplan-Meier survival curves was determined using the Log-rank (Mantel-Cox) test. N and P values are indicated in each graph or figure legend.

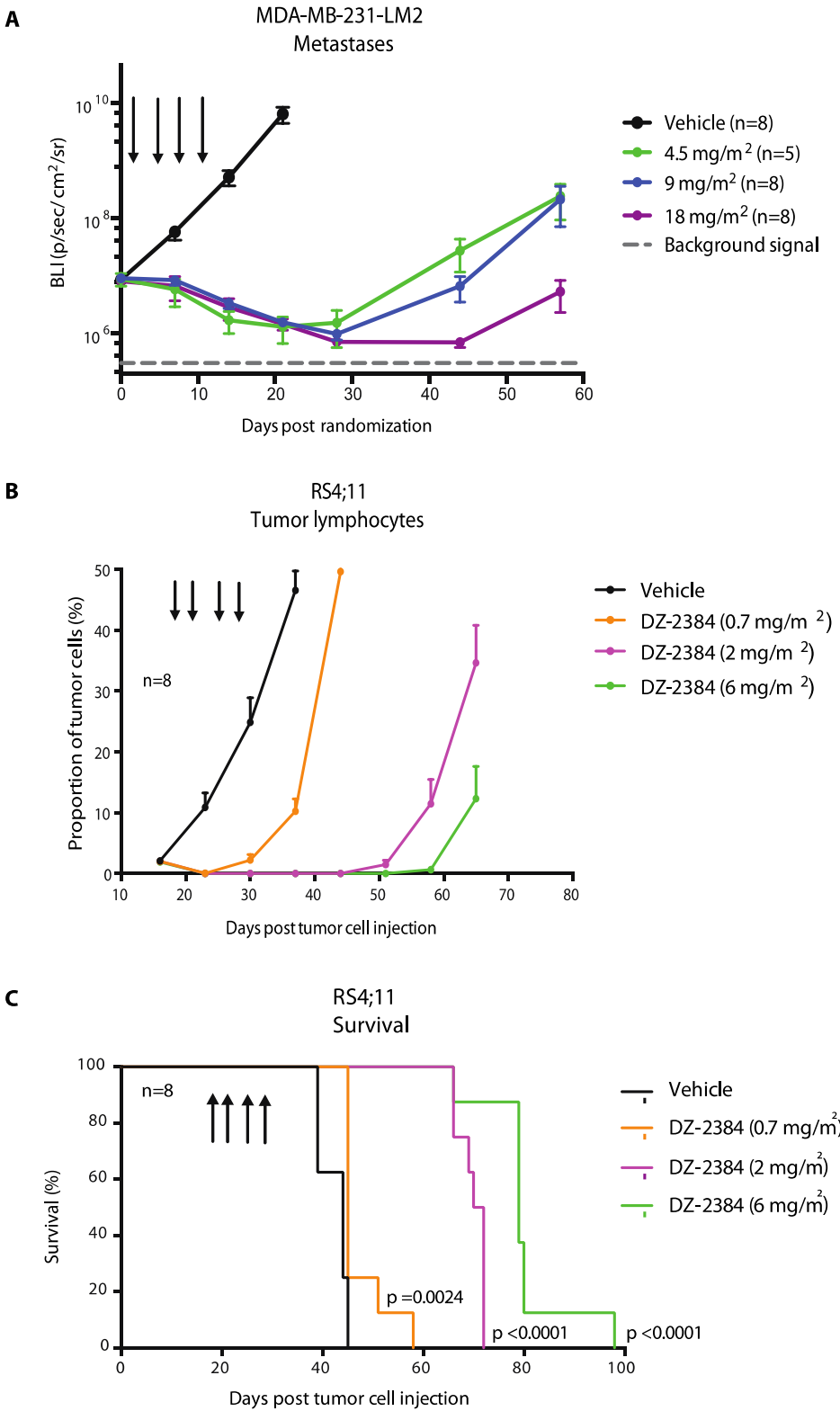
A
MDA-MB-231-LM2
Metastases
BLI (p/sec/ cm2/sr)
Days post randomization
Vehicle (n=8)
4.5 mg/m 2 (n=5)
9 mg/m2 (n=8)
18 mg/m2 (n=8)
Background signal
B
RS4;11
Tumor lymphocytes
Proportion of tumor cells (%)
n=8
Days post tumor cell injection
Vehicle
DZ-2384 (0.7 mg/m 2)
DZ-2384 (2 mg/m 2)
DZ-2384 (6 mg/m 2)
C
RS4;11
Survival
Survival (%)
n=8
p =0.0024
p <0.0001
p <0.0001
Days post tumor cell injection
Vehicle
DZ-2384 (0.7 mg/m2)
DZ-2384 (2 mg/m2)
DZ-2384 (6 mg/m2)

Fig. S1. Antitumor efficacy of DZ-2384 in metastatic breast and adult ALL models. (**A**) Plots show a quantification of the luminescence signal from MDA-MB-231-LM2 lung metastases as a function of time, where arrows denote treatment days. Error bars represent mean ± SEM (n= 8 for all groups except 4.5 mg/m^2, n=5) (**B**) RS4;11 adult ALL tumor cell burden quantified by FACS analysis and represented as the proportion (%) of hCD45 to total circulating white blood (mCD45) cells in each mouse. Bolus iv treatments indicated by arrows. Error bars represent mean ± SEM. (**C**) Kaplan-Meier curves showing survival of mice with systemic RS4;11. P values were determined by Log-rank (Mantel-Cox) test relative to vehicle-treated animals.

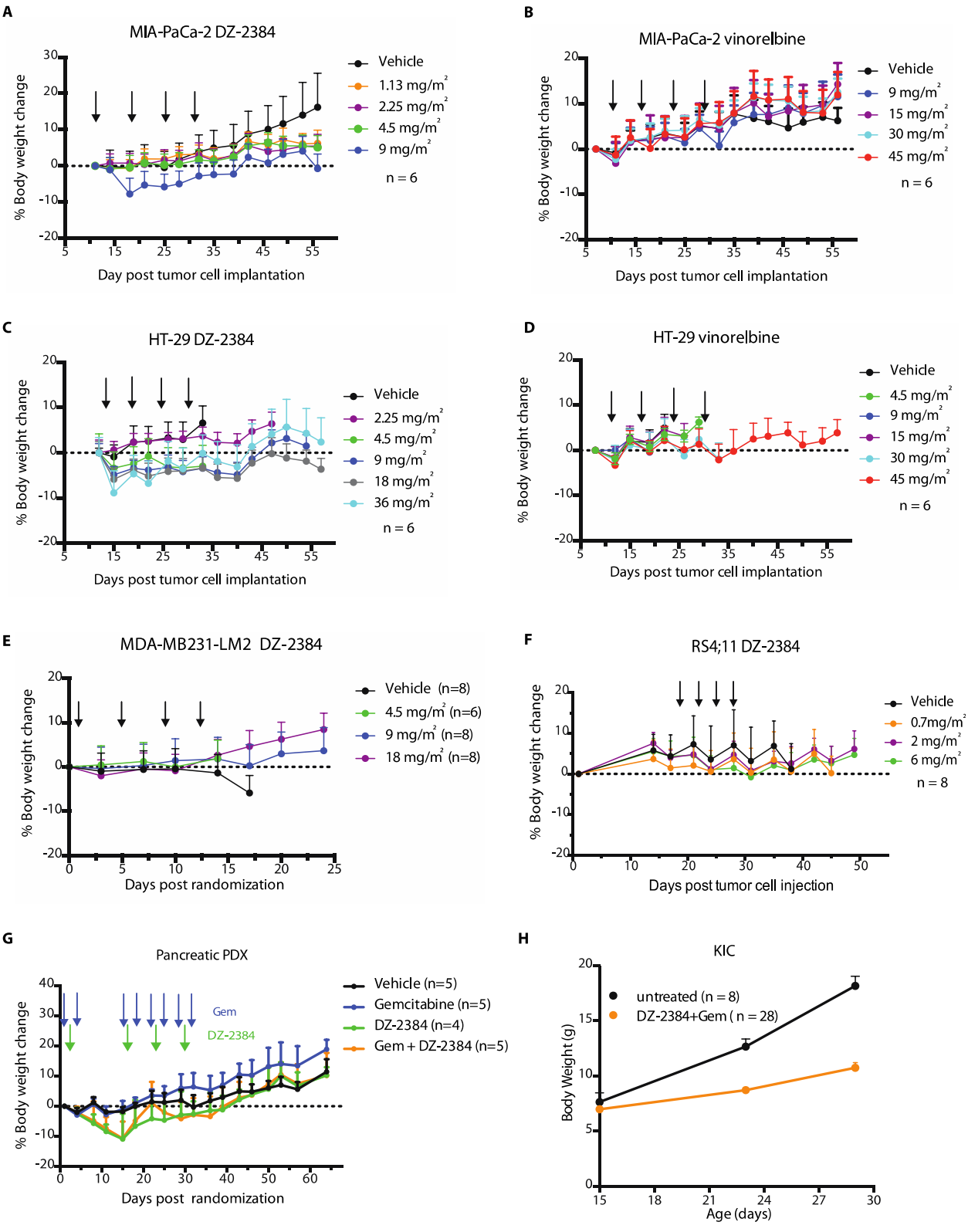
A
MIA-PaCa-2 DZ-2384
% Body weight change
Day post tumor cell implantation
Vehicle
1.13 mg/m2
2.25 mg/m2
4.5 mg/m2
9 mg/m2
n = 6
B
MIA-PaCa-2 vinorelbine
% Body weight change
Days post tumor cell implantation
Vehicle
9 mg/m2
15 mg/m2
30 mg/m2
45 mg/m2
n = 6
C
HT-29 DZ-2384
% Body weight change
Days post tumor cell implantation
Vehicle
2.25 mg/m2
4.5 mg/m2
9 mg/m2
18 mg/m2
36 mg/m2
n = 6
D
HT-29 vinorelbine
% Body weight change
Days post tumor cell implantation
Vehicle
4.5 mg/m2
9 mg/m2
15 mg/m2
30 mg/m2
45 mg/m2
n = 6
E
MDA-MB231-LM2 DZ-2384
% Body weight change
Days post randomization
Vehicle (n=8)
4.5 mg/m2 (n=6)
9 mg/m2 (n=8)
18 mg/m2 (n=8)
F
RS4;11 DZ-2384
% Body weight change
Days post tumor cell injection
Vehicle
0.7mg/m2
2 mg/m2
6 mg/m2
n = 8
G
Pancreatic PDX
% Body weight change
Days post randomization
Gem
DZ-2384
Vehicle (n=5)
Gemcitabine (n=5)
DZ-2384 (n=4)
Gem + DZ-2384 (n=5)
H
KIC
Body Weight (g)
Age (days)
untreated (n = 8)
DZ-2384+Gem (n = 28)

Fig. S2. Body weight in murine xenografts after administration of DZ-2384, vinorelbine, or DZ-2384 and gemcitabine. (**A**-**F**) Percentage body weight change relative to weights at randomization in MIA PaCa-2 (A, B), HT-29 (C, D), MDA-MB-231-LM2 (E), or RS4;11 (F) models treated with DZ-2384 (A, C, E, and F) or vinorelbine (B, D). DZ-2384 was administered iv once (A, C) or twice weekly (E, F) as indicated by arrows. Vinorelbine was administered iv once weekly as indicated by arrows (B, D). (**G**) Percentage body weight change relative to weight at randomization in a pancreatic PDX model treated with 100 mg/m^2 gemcitabine twice weekly, 36 mg/m^2 DZ-2384 at the start of treatment and then once weekly starting two weeks later (see arrows), or the two in combination. *n* = 5 (except DZ-2384: n = 4). (**H**) KIC mice were treated with gemcitabine thrice weekly (Gem) at 37.5 mg/m^2 starting at P15 and with DZ-2384 at 7.5 mg/m^2 (day P16) and 30 mg/m^2 (day P23) according to the schedule in Fig. 1F. All body weights are plotted as the mean +/- SEM.

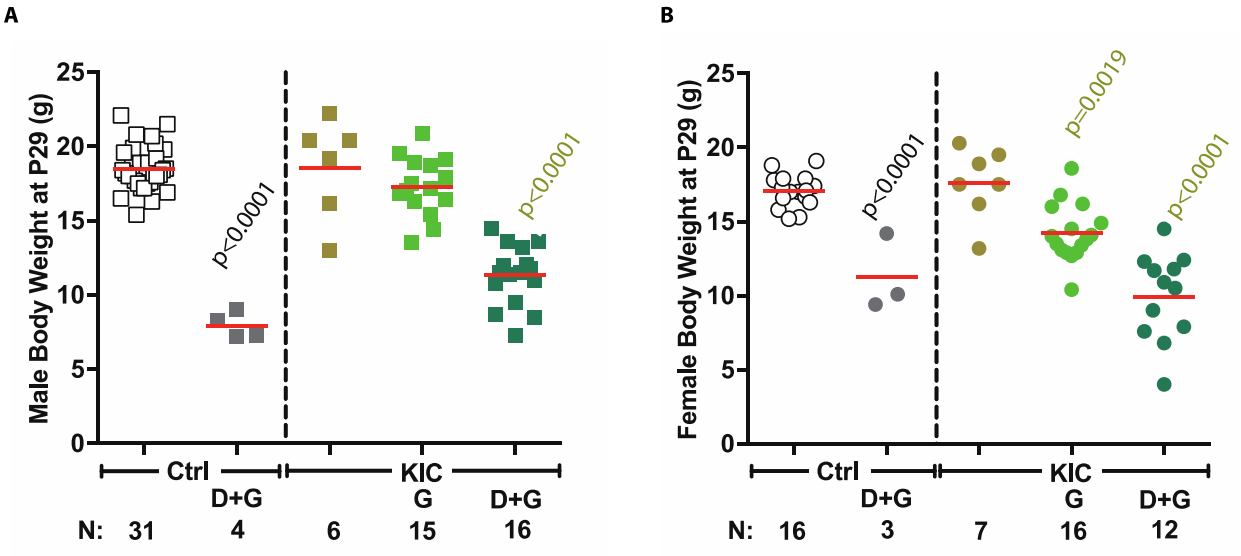

Fig. S3. Body weights of weanling control and *Rgs16::GFP;KIC* mice treated with DZ-2384 and gemcitabine on P29. Body weights of (**A**) male and (**B**) female control (Ctrl) and *Rgs16::GFP;KIC* mice untreated, or treated with gemcitabine thrice weekly at 37.5 mg/m^2 starting at P15 alone (G) or with DZ-2384 (D+G) at 7.5 mg/m^2 (day P16) and 30 mg/m^2 (day P23) according to the schedule in Fig. 1F. Horizontal red lines show the mean of each group.

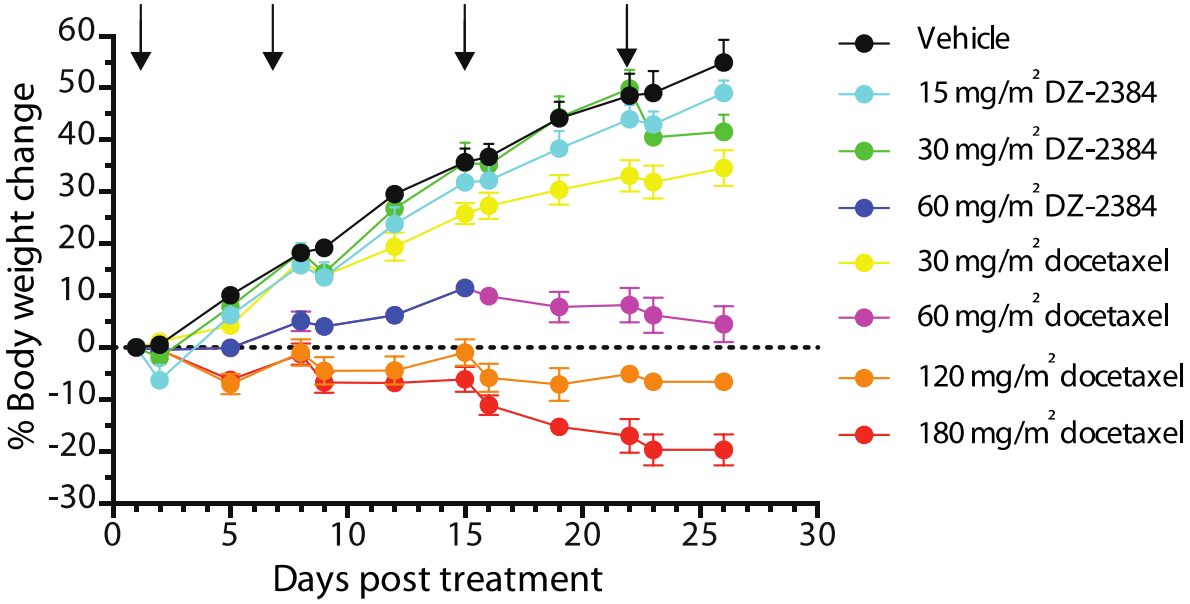

Fig. S4. Body weight change in rats administered DZ-2384 or docetaxel weekly for 4 weeks. Sprague Dawley rats received DZ-2384 or docetaxel iv bolus at the indicated doses once weekly for 4 weeks (marked by arrows). Body weights are represented as percentage change relative to day 1 of treatment and correspond to mean +/- SEM, n=5. 60 mg/m^2 DZ-2384 curve is discontinued after day 16 for the 60 mg/m^2 dose of DZ-2384 due to the death of 2 animals.

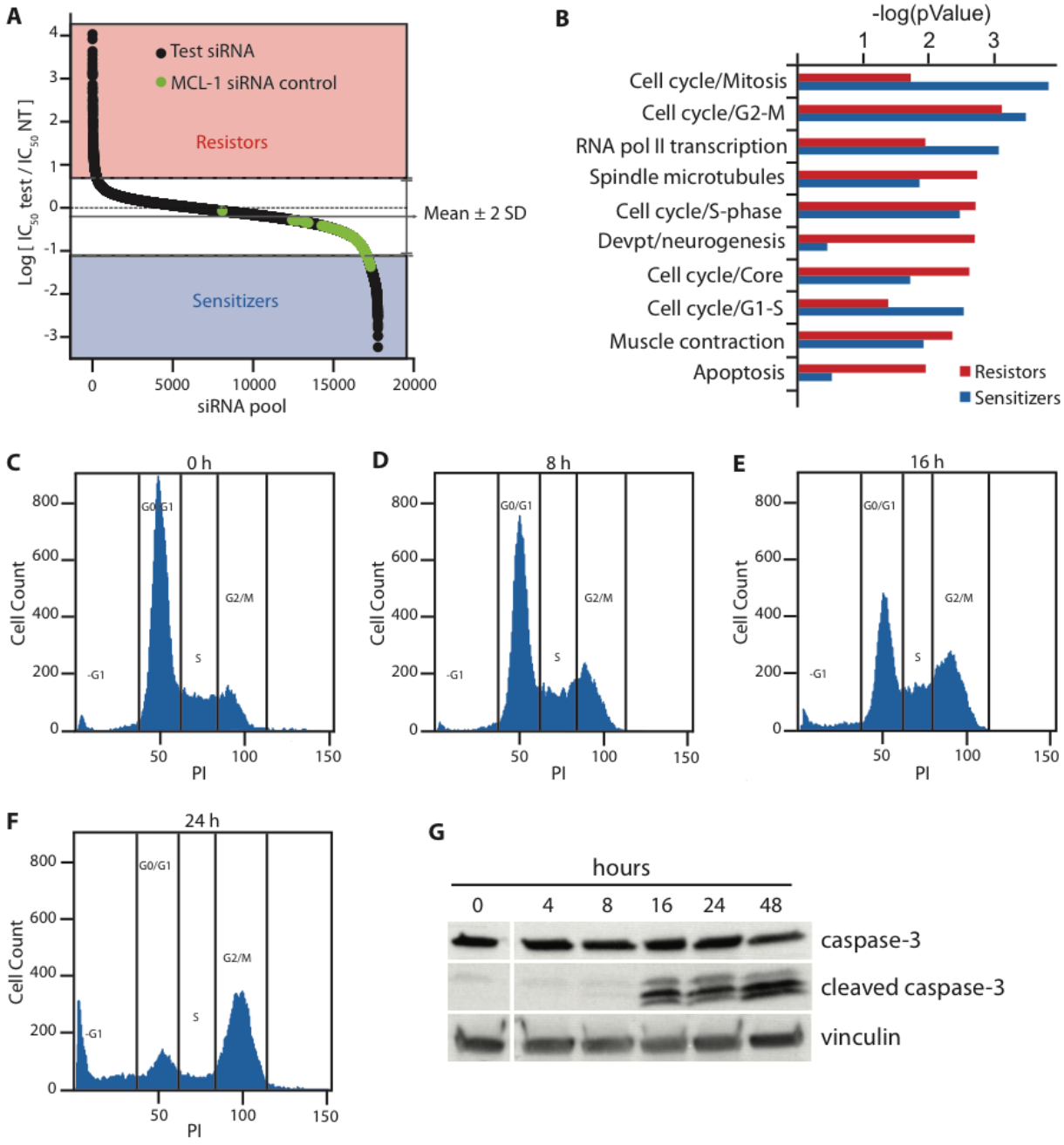
A
Test siRNA
MCL-1 siRNA control
Resistors
Sensitizers
Mean ± 2 SD
Log [IC50 test / IC50 NT]
siRNA pool
B
-log(pValue)
Cell cycle/Mitosis
Cell cycle/G2-M
RNA pol II transcription
Spindle microtubules
Cell cycle/S-phase
Devpt/neurogenesis
Cell cycle/Core
Cell cycle/G1-S
Muscle contraction
Apoptosis
Resistors
Sensitizers
C
0 h
D
8 h
E
16 h
F
24 h
Cell Count
PI
G0/G1
G2/M
S
G1
G
hours
0
4
8
16
24
48
caspase-3
cleaved caspase-3
vinculin

Fig. S5. Functional genomic screen and cell cycle regulation as the DZ-2384 mechanism of action. (**A**) H1299 cells were transfected with a genome-wide siRNA library in individual wells and 48 h later treated with a dose range of DZ-2384. Viability was measured by CellTiter-Glo after 72 h of treatment. The IC_{50} for test siRNAs are expressed relative to the mean IC_{50} obtained for four non-targeting (NT) siRNAs from each screen plate and are represented in rank order on a log scale. *MCL-1* siRNA was used as a positive control sensitizer. Sensitizer and resistor hits were classified as > 2 SD away from the mean. (**B**) Rank order list of the most statistically enriched process networks from among the sensitizer and resistor gene sets (GeneGo Pathway Analysis, Metacore). (**C**-**F**) Flow cytometric histograms of H1299 cells stained with propidium iodide (C) before treatment and (D) 8 h, (E) 16 h, or (F) 24 h after treatment with 100 nM DZ-2384. (**G**) Western blot analysis of inactive and activated caspase-3 in H1299 cell extracts treated with 100 nM DZ-2384 for the indicated times. Vinculin immunodetection shows equal protein loading.

A DZ-2384

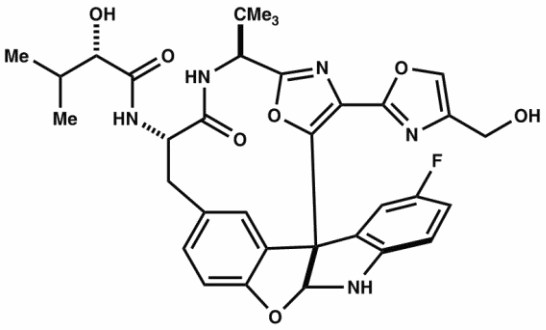

[IC_{50}] H1299: 12 nM

B DZ-2384D

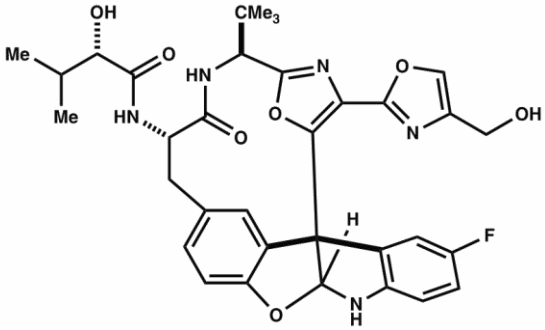

[IC_{50}] H1299: 822 nM

Fig. S6. DZ-2384 and inactive DZ-2384D compound structures. Molecular structures of DZ-2384 (**A**) and inactive DZ-2384D (**B**) compounds. IC_{50} values represent viability of H1299 cells in a 3-day CellTiter-Glo assay.

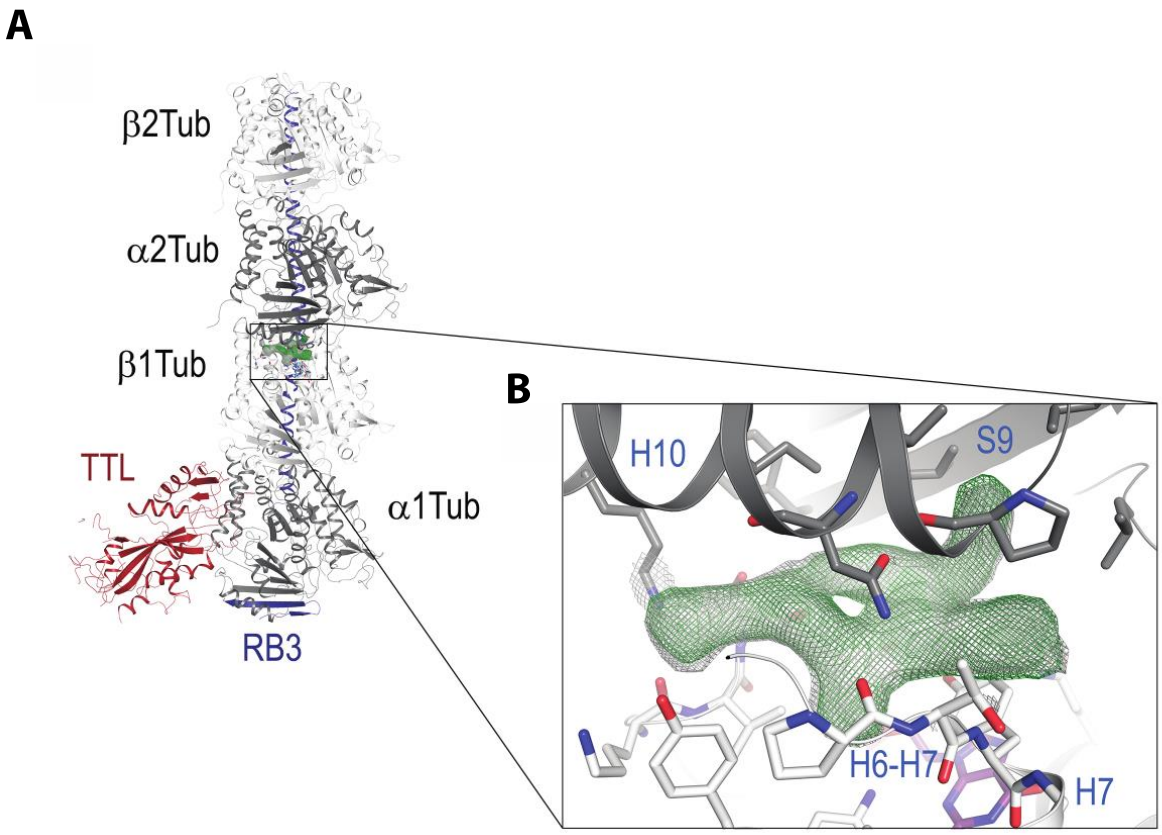

Fig. S7. X-ray crystal structure of T_2R-TTL in complex with DZ-2384. (**A**) Overall view of the DZ-2384-T_2R-TTL complex. The tubulin subunits (α-tubulin; dark gray and β-tubulin; light gray), RB3 (blue), and TTL (red) are shown in ribbon representation and are labeled; the simulated annealing omit map at the interdimer interface is depicted in green. The boxed section is enlarged in (**B**). (B) Simulated annealing omit map of DZ-2384. The SigmaA-weighted 2mFo-DFc (gray mesh) and mFo-DFc (green mesh) electron density maps are contoured at 1.0σ and +/- 3.0σ, respectively. The interacting residues of α- and β-tubulin are in stick representation and are colored according to the same color code as in (A). The secondary structural elements are in ribbon representation and are labeled.

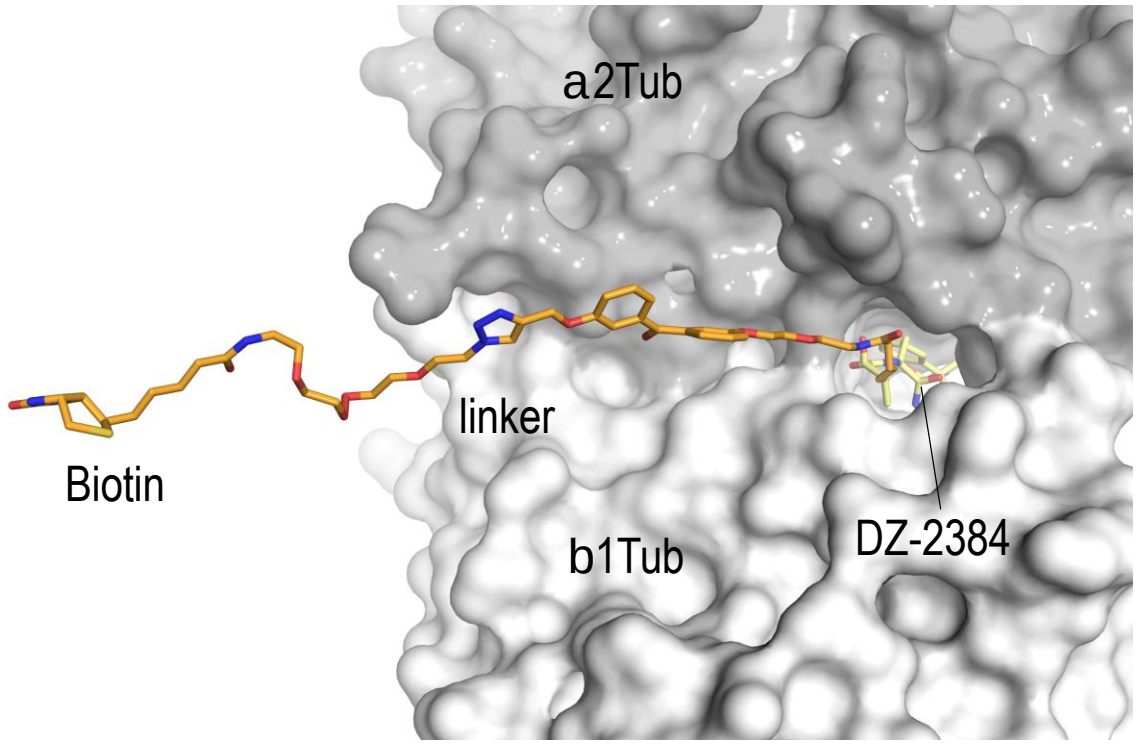

Fig. S8. Model of biotinylated DZ-2384 binding to tubulin in the context of T_2R-TTL. View into the tubulin interdimer interface of the T_2R-TTL complex highlighting that biotinylation of DZ-2384 does not interfere with ligand binding. The α2- and β1-tubulin chains are displayed as dark and light gray surfaces, respectively. The DZ-2384 (yellow) and the biotin/linker (orange) moieties are in stick representation and are labeled.

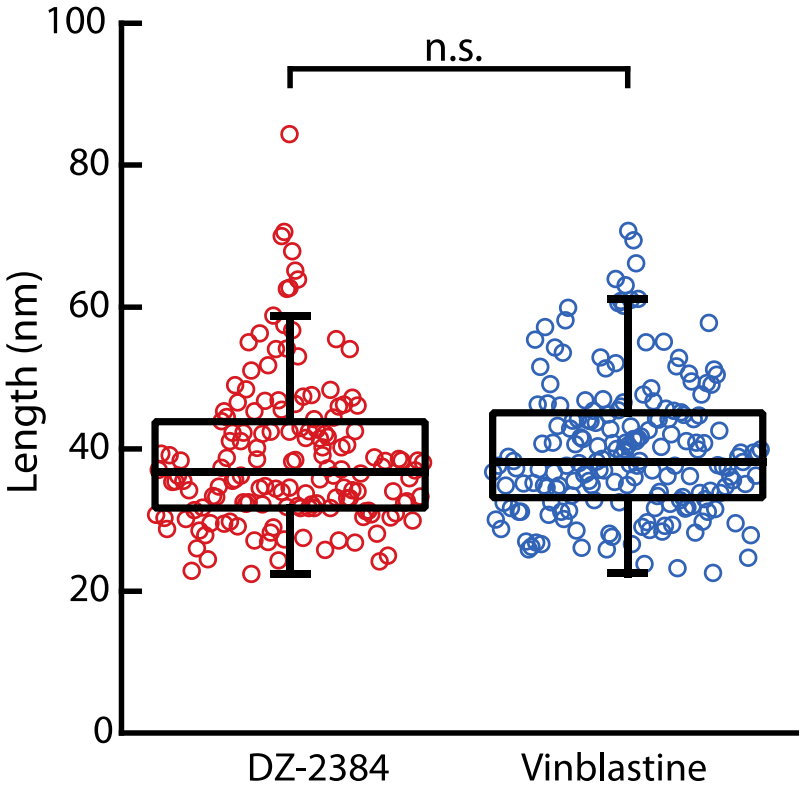

Fig. S9. Tubulin oligomer lengths measured during curvature analysis. Box plot showing the measured lengths of the DZ-2384 oligomers (left) and vinblastine oligomers (right) observed by cryo-electron microscopy. Statistical difference calculated using Welch's t-test; n.s.: no significant difference observed.

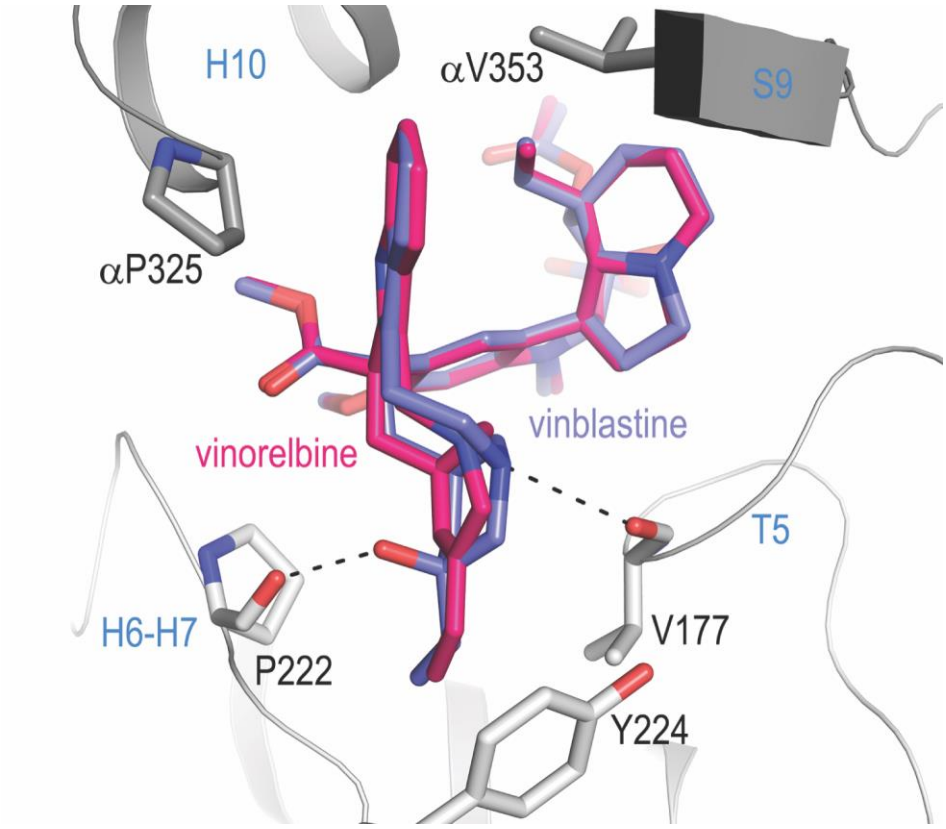

Fig. S10. Modeled comparison of vinblastine and vinorelbine binding to tubulin. Superposition of vinorelbine (model, pink) onto the crystal structure of vinblastine (blue) in complex with tubulin [PDB-ID 4EB6 (*67*)]. The key interacting structural elements of α- and β-tubulin are in gray and white ribbon and stick representation and are labeled. The two hydrogen bonds that are formed by vinblastine to the main chain carbonyls of Val177 and Pro222 (black dashed lines) are likely absent in the case of vinorelbine binding.

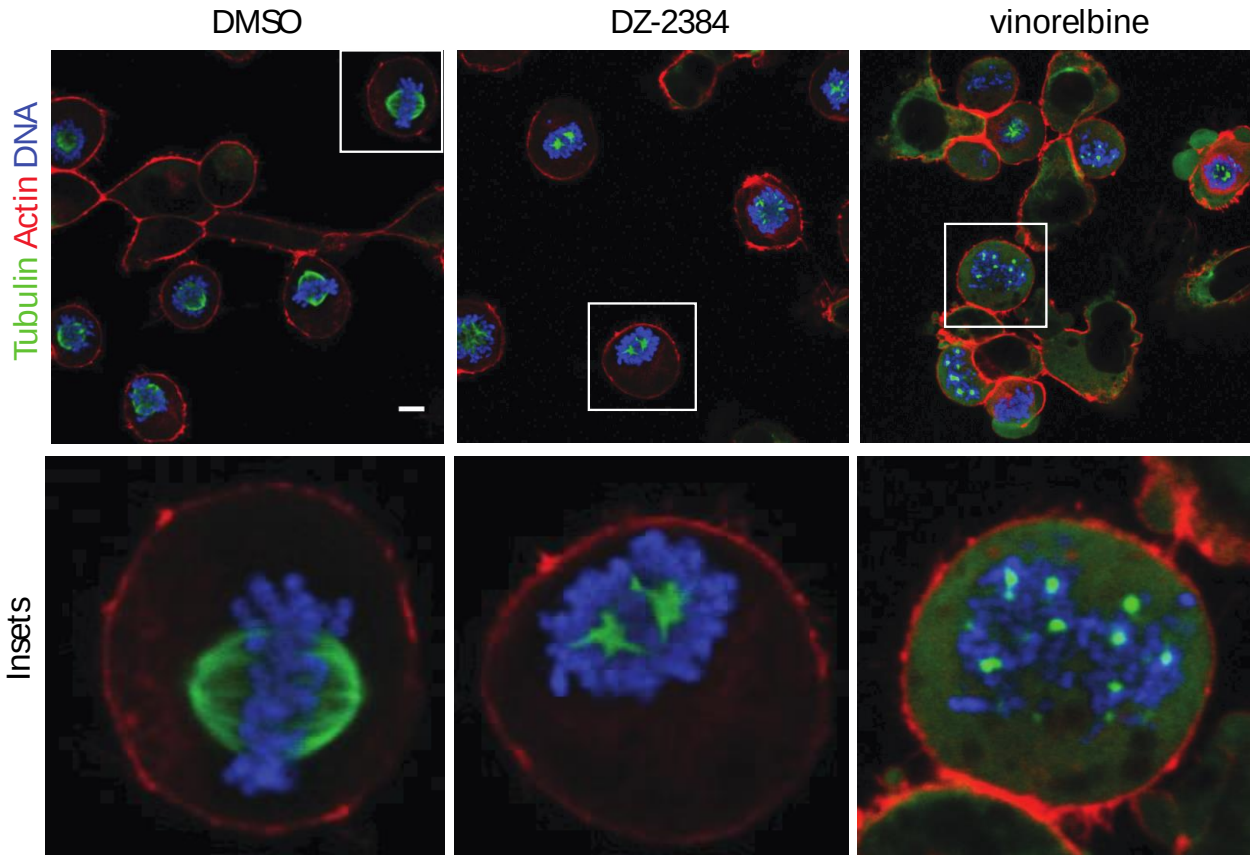

Fig. S11. The effects of DZ-2384 and vinorelbine on mitotic H1299 cells. H1299 cells were synchronized with RO-3306, then washed and released in DMSO (left panel), or the IC_{80} of DZ-2384 (center) and vinorelbine (right) (100 nM and 80 nM, respectively) for 1 h before fixation. Samples were immunostained with an antibody to α-tubulin (green), phalloidin (red, to detect actin), or DAPI (blue). Images were acquired by confocal microscopy. Scale bar: 10 μm. Insets show an enlargement of single cells (bottom three panels).

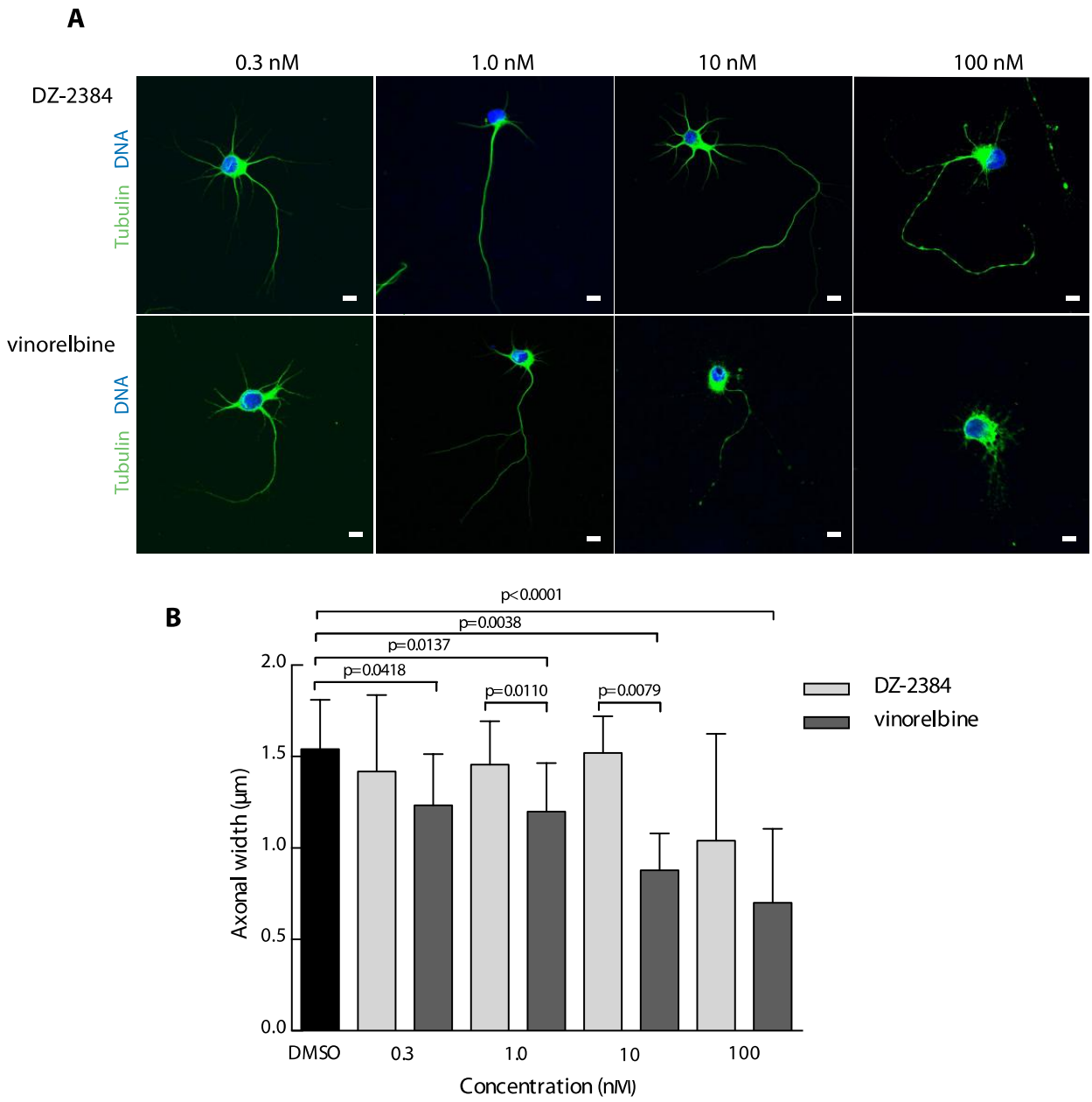

Fig. S12. Axon width of E18 rat cortical neurons treated with DZ-2384 and vinorelbine. Treatment of E18 rat primary cortical neurons with 0.3 (n=11), 1 (n=10), 10 (n=5), and 100 nM (n=7) of DZ-2384 or 0.3 (n=9), 1 (n=15), 10 (n=5), and 100 nM (n=9) vinorelbine for 1 h. (**A**) Cells are immunostained with an α-tubulin antibody (green), and nuclei are stained with DAPI (blue). Scale bars: 10 µm. (**B**) Axon width was quantified using Image J. Mean ± SEM are represented. All p values are indicated for statistically different groups and were determined using a non-paired two-tailed non-parametric student's t-test (Mann-Whitney).

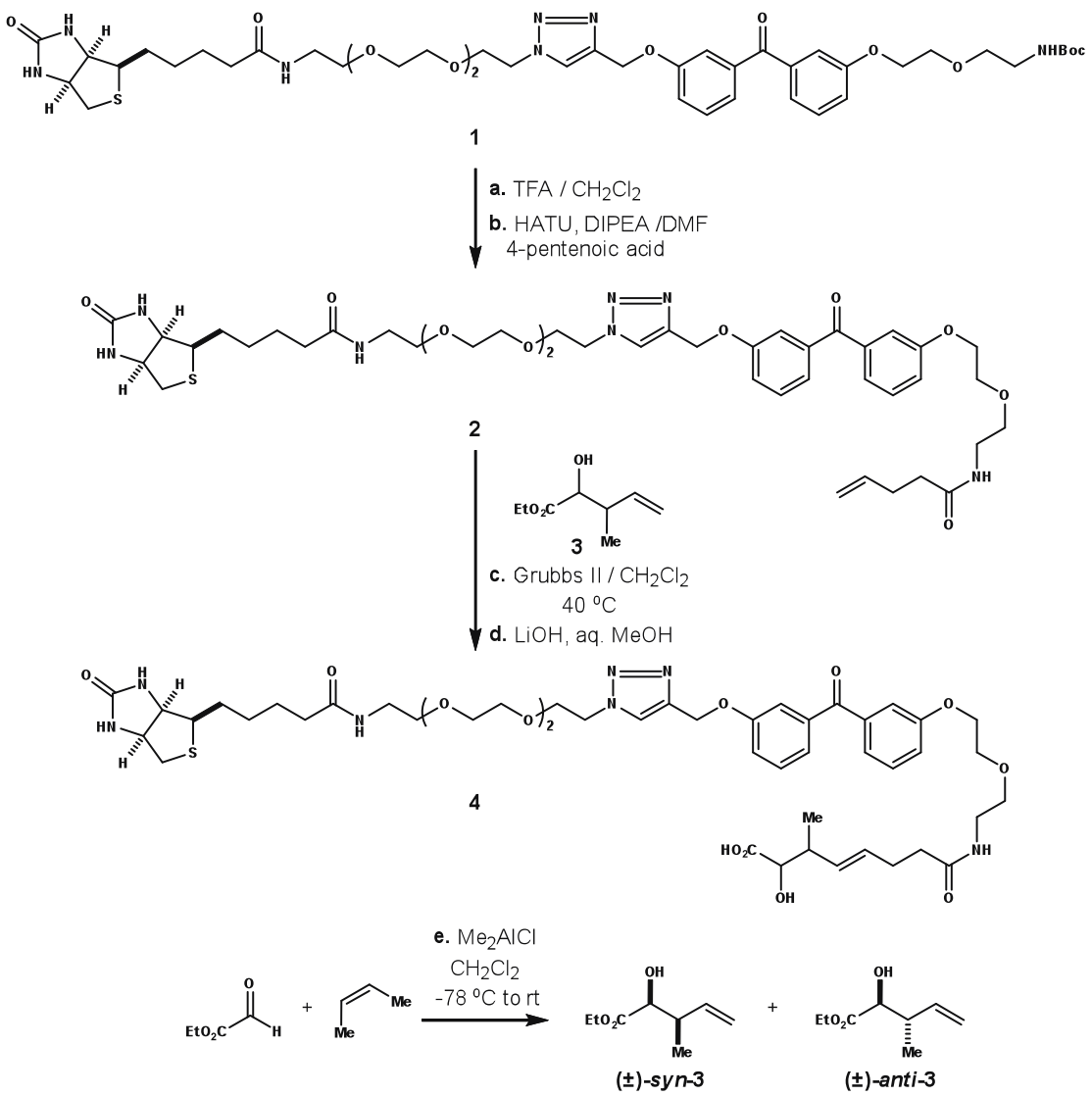

Fig. S13. Preparation of an extended, multipurpose diazonamide side chain harboring a biotin tag. Reagents and conditions: **a**. TFA-DCM (1:3), RT, 100 min. **b**. HATU, DIPEA, 4-pentenoic acid, DMF, 2 h, 60% from 1. **c**. Grubbs II 40°C, 20 h. **d**. LiOH hydrate, aq. MeOH, 1 h, then HPLC purification, 18% from 2. **e**. Ethyl glyoxylate, DCM, Me2AlCl (1.0 M hexanes), -78°C to RT, 20 h, 20%. TFA = trifluoroacetic acid, DCM = dichloromethane, HATU = 1-[bis(dimethylamino)methylene]-1H-1, 2, 3-triazolo[4,5-b]pyridinium-3-oxid hexa-fluorophosphate, DIPEA = N, N-diisopropylethylamine, DMF = dimethylformamide, Grubbs II = 2nd generation Grubbs metathesis catalyst.

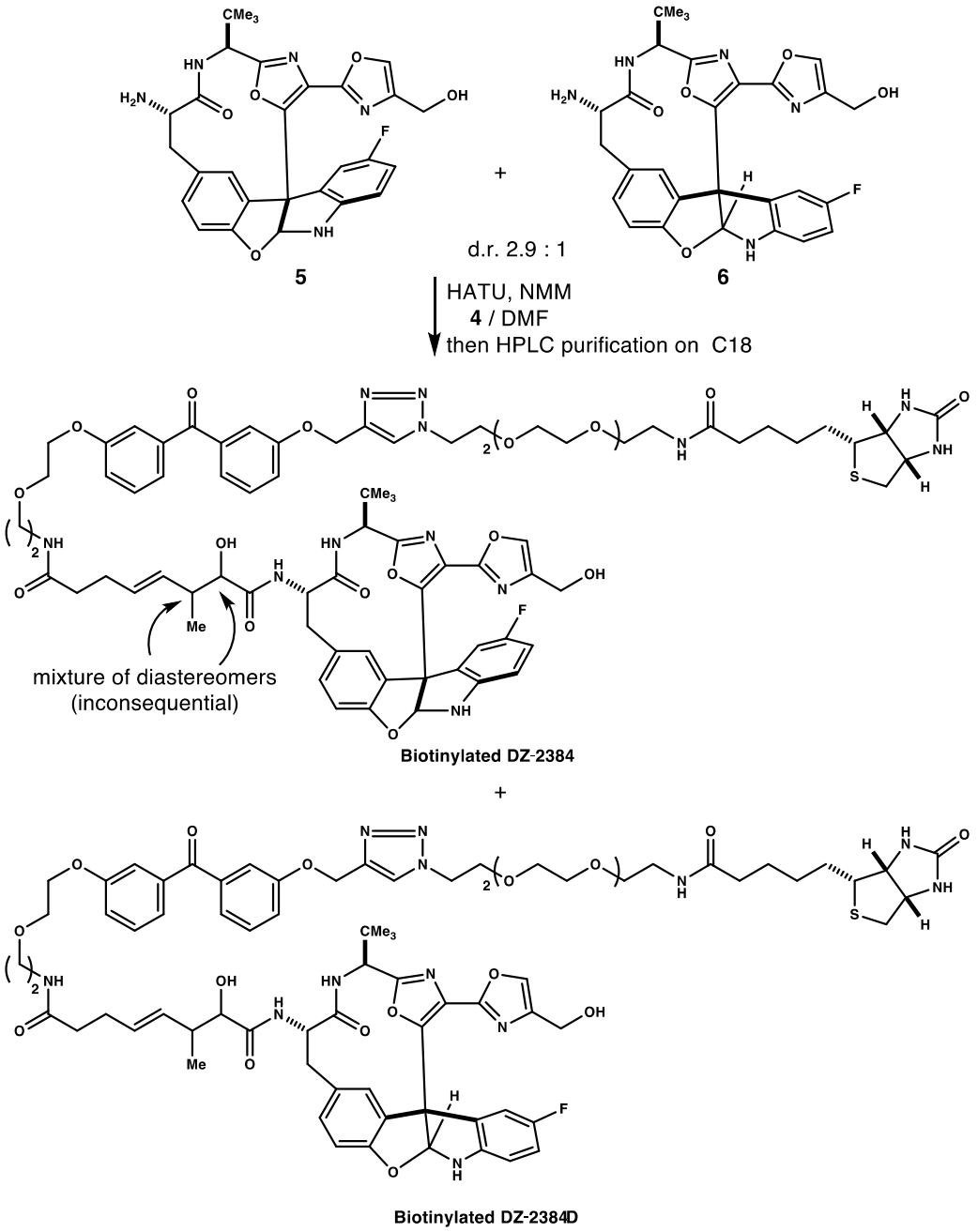

Fig. S14. Conjugation of extended side chain 4 with diastereoisomeric diazonamide core structures. Reagents and conditions: 4, HATU, NMM, DMF, 20 h. NMM = N-methylmorpholine.

Table S1. Survival of DZ-2384–treated and vinorelbine-treated mice bearing HT-29 tumors.

Compound	Dose (mg/m^2)	Mean survival (days +/- SD)	P value*	Median survival (days)	Efficacy** (%T/C)
DZ-2384	**Vehicle**	42.7 ± 6.6	-	41.5	100
	2.25	55.5 ± 11.0	0.0550	50	120
	4.5	53.8 ± 12.4	0.0456	61	147
	9	64.3 ± 7.0	0.0007	68	164
	18	74.2 ± 9.7	0.0007	74.5	180
	36	67.0 ± 31.0	0.0146	65	157
Vinorelbine	**Vehicle**	35.5 ±12.2	-	32.5	100
	4.5	47.2 ± 24.4	0.8339	39.5	122
	9	39.2 ± 11.5	0.7169	41.5	128
	15	51.5 ± 23.8	0.2349	46.5	143
	30	53.7 ± 15.2	0.0655	52.0	160
	45	57.8 ± 22.9	0.0201	62.5	192

*Statistical differences in mean survival were calculated with student's t-test. N=6 for all test groups.
**Efficacy is expressed as a percentage (%T/C), where T=median survival time of animals treated with drug and C = median survival time of vehicle-treated animals.

Table S2. Summary of clinical observations in *Rgs16::GFP;KIC* mice administered DZ-2384 and gemcitabine.

Clinical observations	Untreated (n=46)	Gemcitabine* (n=31)	DZ-2384** + gemcitabine (n=28)
Diarrhea	0/46	0/31	1/28
Hind limb paralysis	0/46	0/31	1/28
Mild hair loss	0/46	0/31	3/28
Death	0/46	0/31	0/28

Mice observed until sacrifice at day P29.
*Gemcitabine was administered ip at 37.5 mg/m^2 thrice weekly starting at P15.
**DZ-2384 was administered ip at 7.5 mg/m^2 on day P16 and at 30 mg/m^2 on day P23.

Table S3. Summary of lethality in *Rgs16::GFP;KIC* mice and littermates administered DZ-2384.

DZ-2384* (mg/m^2)	Mouse age at administration	Total number of littermates (KIC mice)	Incidence of death after 24 h
7.5**	P16	35 (28)	0/35
15***	P15	16 (2)	0/16
24	P16	10 (0)	1/10
30	P16	10 (0)	5/10

*administered ip.
**after gemcitabine (37 mg/m^2) administered at P15.
***5 mice died before P29.

Table S4. Summary of the effects of DZ-2384 on mouse bone marrow.

Bone marrow parameter	Vehicle	36 mg/m^2 NOAEL		48 mg/m^2 MTD	
	Mean (SD)	**Mean (SD)**	**P value**	**Mean (SD)**	**P value**
M/E	1.07 (0.19)	1.24 (0.15)	0.294	1.26 (0.27)	0.381
	Incidence of abnormal results				
Ery	0/3	0/3		0/3	
Mye	0/3	0/3		0/3	
MGR	0/3	0/3		0/3	
L/M	0/3	0/3		0/3	
Eosinophils	0/3	0/3		0/3	
Plasma cells	0/3	0/3		0/3	
Megakaryocytes	0/3	0/3		0/3	
Comments	No morphological abnormalities	No morphological abnormalities		No morphological abnormalities	

N=3 animals per treatment group. P value determined by student's t test relative to vehicle control.

M/E = myeloid to erythroid ratio, Ery = synchronicity of erythroid series cell development, Mye= synchronicity of granulocytic series cell development, MGR = marrow granulocyte reserve composed of segmented neutrophils and bands, L/M = mononuclear cells.

Table S5. Summary of the effects of vinorelbine on mouse bone marrow.

Bone marrow parameter	Vehicle	30 mg/m^2 NOAEL		45 mg/m^2		60 mg/m^2		75 mg/m^2 MTD	
	Mean (SD)	Mean (SD)	P value	Mean (SD)	P value	Mean (SD)	P value	Mean (SD)	P value
M/E	1.06 (0.23)	1.49 (0.27)	0.105	2.49 (0.66)	0.052	2.15 (0.51)	0.048	6.30 (4.58)	0.186
	Incidence of abnormal results								
Ery	0/3	0/3		0/3		0/3		0/3	
Mye	0/3	0/3		0/3		0/3		0/3	
MGR	0/3	0/3		0/3		0/3		0/3	
L/M	0/3	0/3		0/3		0/3		0/3	
Eosinophils	0/3	0/3		0/3		0/3		0/3	
Plasma cells	0/3	0/3		0/3		0/3		0/3	
Megakary-ocytes	0/3	0/3		0/3		0/3		0/3	
Comments	No morpho-logical abnormalities	No morphological abnormalities		2/3 moderate granulocytic hyperplasia		2/3 moderate granulocytic hyperplasia		3/3 moderate - marked granulocytic hyperplasia	

N=3 animals per treatment group. P value determined by student's t test relative to vehicle control.

M/E = myeloid to erythroid ratio, Ery = synchronicity of erythroid series cell development, Mye= synchronicity of granulocytic series cell development, MGR = marrow granulocyte reserve composed of segmented neutrophils and bands, L/M = mononuclear cells. P value determined by student's t test relative to vehicle control.

Table S6. Microscopic changes in dorsal root ganglia and sciatic nerves of rats treated with DZ-2384 and docetaxel.

Compound	**Vehicle**		**DZ-2384**				**Docetaxel**	
Dose (mg/m^2/week)*			**12**		**30**		**120**	
Day scored	**24**	**44**	**24**	**44**	**24**	**44**	**24**	**44**
Number of rats	n=7	n=5	n=7	n=5	n=7	n=5	n=7	n=5
Dorsal root ganglia *Degeneration, neuron*								
Minimal	0/7	0/5	0/7	0/5	1/7	0/5	7/7	4/5
Degeneration, axon								
Minimal	0/7	0/5	0/7	0/5	2/7	0/5	5/7	5/5
Mild	0/7	0/5	0/7	0/5	0/7	0/5	2/7	0/5
Sciatic nerve *Degeneration, axon*								
Minimal	0/7	0/5	0/7	0/5	3/7	0/5	0/7	0/5
Mild	0/7	0/5	0/7	0/5	0/7	0/5	6/7	5/5
Moderate	0/7	0/5	0/7	0/5	0/7	0/5	1/7	0/5

*DZ-2384 and docetaxel i.v. once weekly for 4 weeks.

Table S7. X-ray crystallography data collection and refinement statistics.

Data collection[a]	**DZ-2384-T_2R-TTL**
Space group	$P2_12_12_1$
Cell dimensions	
a, b, c *(Å)*	103.2, 154.7, 180.3
Resolution (Å)	77.4 – 2.40 (2.46 – 2.40)
R_{meas} ***(%)***	11.5 (423.1)
R_{pim} ***(%)***	3.9 (123.6)
$CC_{1/2}$[b]	100.0 (32.9)
I/σI	18.6 (0.75)
Completeness (%)	99.8 (99.7)
Redundancy	13.6 (13.5)
Refinement	
Resolution (Å)	77.4 – 2.40
No. unique reflections	112921
R_{work}/R_{free} ***(%)***	18.8 / 24.2
Average B-factors (Å²)	
Complex	84.1
Solvent	66.0
Ligand	60.3
Wilson B-factor	64.8
Root mean square deviation from ideality	
Bond length (Å)	0.004
Bond angles (°)	0.788
Ramachandran statistics[c]	
Favored regions (%)	95.55
Allowed regions (%)	4.4
Outliers (%)	0.05

[a]Highest shell statistics are in parentheses. [b]$CC_{1/2}$= percentage of correlation between intensities from random half-datasets(*14*). [c]As defined by MolProbity(*15*).

Movie S1. Microtubule growing ends in U-2OS cells: vehicle control. U-2OS cells expressing EB3-mcherry were seeded in an experimental chamber U-slide and treated with vehicle control (0.2 % DMSO) (movie S1), DZ-2384 (movie S2) and vinorelbine (movie S3). Live cell images were acquired starting at 3 minutes by spinning disc confocal microscopy over the course of 1 min.

Movie S2. The effect of treatment on microtubule growing ends in U-2OS cells: DZ-2384. U-2OS cells were seeded and photographed as in the legend for movie S1. Cells were treated with DZ-2384 at IC_{80} (400 nM).

Movie S3. The effect of treatment on microtubule growing ends in U-2OS cells: vinorelbine. U-2OS cells were seeded and photographed as in the legend for movie S1. Cells were treated with vinorelbine at IC_{80} (150 nM).